ORIGINAL PAPER

Towards high-efficiency CZTS solar cell through buffer layer optimization

Farjana Akter Jhuma[1] · Marshia Zaman Shaily[1] · Mohammad Junaebur Rashid[1]

Abstract

Cu_2ZnSnS_4 (CZTS)-based solar cells show a promising performance in the field of sunlight-based energy production system. To increase the performance of CZTS-based solar cell, buffer layer optimization is still an obstacle. In this work, numerical simulations were performed on structures based on CZTS absorber layer, ZnO window layer, and transparent conducting layer n-ITO with different buffer layers using SCAPS-1D software to find a suitable buffer layer. Cadmium sulfide (CdS), zinc sulfide (ZnS) and their alloy cadmium zinc sulfide ($Cd_{0.4}Zn_{0.6}S$) were used as potential buffer layers to investigate the effect of buffer thickness, absorber thickness and temperature on open-circuit voltage (V_{oc}), short-circuit current (J_{sc}), fill factor (FF) and efficiency (η) of the solar cell. The optimum efficiencies using these three buffer layers are around 11.20%. Among these three buffers, $Cd_{0.4}Zn_{0.6}S$ is more preferable as CdS suffers from toxicity problem and ZnS shows drastic change in performance parameters. The simulation results can give important guideline for the fabrication of high-efficiency CZTS solar cell.

Introduction

The green, clean, renewable and sustainable energy source, sun has a very high potential to meet up the electricity demand of the world and the sunlight can directly be converted to electricity through solar cell using the principle known as photovoltaic (PV) effect. To obtain low cost and high-efficiency solar cell, researchers are working on many different solar materials such as Si, CdTe, Cu(In,Ga)Se_2 (CIGS), Cu_2ZnSnS_4 (CZTS), CZTSSe and organic resources [1, 2].

The most widely used Si-based solar cell exhibits high conversion efficiency (up to 24.5% at the University of New South Wales) [3]. However, it suffers from low throughput and high cost, therefore, could not affect the world's energy market [4]. On the other hand, CIGS and CdTe offer high efficiencies (around 21% and 21%, respectively) for which they attracted the researchers for the last few years [5]. The main problem with these two materials is the toxicity of the constituent materials cadmium and selenium and also the less availability of tellurium and indium on earth [6]. To meet up the problems, an alternative material, CZTS has drawn the attraction with good advantages over CIGS and CdTe. During last few years, a good amount of researches had been done to improve the solar cell efficiency using CZTS absorber layer [7]. Wei Wang et al. presented a record cell efficiency of around 12.6% using a hydrazine pure solution approach for Cu_2ZnSnS_4-based solar cell [8].

The material CZTS is a quaternary semiconductor with two different crystal structures stannite and kesterite. Kesterite structure shows more stability than stannite structure [9]. One important advantage of CZTS is that it consists of earth-abundant materials which are non-toxic. Thus, CZTS offers lower cost in comparison with other thin-film solar cell that makes it more promising in PV technology. CZTS shows excellent photovoltaic properties such as a direct bandgap with bandgap energy of 1.45–1.6 eV and absorption coefficient over $1 \times 10^4 \, cm^{-1}$ [10]. CZTS can be fabricated using

✉ Farjana Akter Jhuma
    jhuma.univdhaka@gmail.com

    Marshia Zaman Shaily
    marshiazaman@gmail.com

    Mohammad Junaebur Rashid
    mjrashid@du.ac.bd

1   Department of Electrical and Electronic Engineering, University of Dhaka, Dhaka 1000, Bangladesh

different processes such as sputtering, evaporation, spray pyrolysis, electrodeposition, sol–gel technique, etc. [11].

Though CZTS has become a good choice as solar cell material, buffer layer optimization is still an issue for its progress. The buffer layer provides band alignment between the CZTS and window layer and also reduces defects and interfacial strain due to the window layer [12]. Cadmium sulfide (CdS) can be used as a prominent buffer as it improves interface with the absorber CZTS and has higher transmission in the blue wavelength region. It has a bandgap of 2.42 eV and absorbs photons with wavelength lower than 590 nm covering 24% of the solar spectrum [13]. However, CdS contains large amount of Cd which is toxic and also produces a large amount of wastage during the deposition processes. To avoid this problem, an environment friendly material zinc sulfide (ZnS) can also be used as an alternative buffer layer. ZnS has a higher bandgap of 3.5 eV compared to CdS which results in less absorption of low-wavelength photons. It also produces better interface with CZTS creating a potential barrier to separate the electron–hole pair [14].

$Cd_{1-x}Zn_xS$ is another buffer layer which is promising as its bandgap can be varied between 2.42 eV (CdS) and 3.5 eV (ZnS). The bandgap of $Cd_{1-x}Zn_xS$ for different Zn composition (x) can be calculated using the following equation which is a modified Vegard's law [15]:

$$E_g\left(Cd_{1-x}Zn_xS\right) = 2.566 + 0.041x + 1.086x^2 (eV). \tag{1}$$

With increasing Zn concentration, bandgap increases letting lower wavelength photon through the device. Thus, instead of CdS, $Cd_{1-x}Zn_xS$ can be used to obtain a more transparent window in the short-wavelength region, already demonstrated by Oladeji et al. [16]. On the other hand, the grain size decreases as Zn concentration increases in $Cd_{1-x}Zn_xS$ [17]. It turns out that for a Zn content of $x = 0.6$ in $Cd_{1-x}Zn_xS$, highest current density can be achieved which leads to a significant enhancement in the solar cell efficiency [15]. Therefore, in this simulation study, 60% Zn is used in $Cd_{1-x}Zn_xS$ and the bandgap of 2.98 eV is calculated using Eq. (1).

The main objective of this work is to offer a CZTS solar cell with high efficiency using a suitable buffer layer. For this reason, three CZTS solar cell device models using three different buffer layers such as CdS, ZnS, and $Cd_{0.4}Zn_{0.6}S$ were numerically analyzed using SCAPS-1D to obtain the solar cell performance parameters. Different solar cell parameters V_{oc}, J_{sc}, fill factor (FF), and efficiency (η) were observed and performance analysis was conducted between the three structures CdS/CZTS, ZnS/CZTS and $Cd_{0.4}Zn_{0.6}S$/CZTS.

Methodology and device structure

SCAPS-1D, a one-dimensional solar cell simulation software developed at the Department of Electronics and Information Systems (EIS), University of Gent, Belgium, was used for numerically analyzing the solar cell. Up to seven different layers can be added in the cell definition panel of the software which makes it more suitable for solar cell simulation. Physical properties such as bandgap, electron affinity, dielectric permittivity, etc., for different layers can be modified in the layer properties panel which helps to achieve the desired structure. The necessary working point specification can be indicated in the action panel. The software supports grading of all physical parameters and also specification of properties of front and back contact. A large number of AC and DC electrical measurements including short-circuit current density (J_{sc}), fill factor (FF), open-circuit voltage (V_{oc}), conversion efficiency (η), quantum efficiency (QE), spectral response, generation and recombination profile can be calculated as well as displayed using the software SCAPS-1D, compared to other simulation software [18].

Figure 1 shows the solar cell structure used in this study. The structure started with soda lime glass substrate. A thin MoS_2 layer of thickness of 100 nm to avoid high series resistance was used over the absorber layer, as this layer can be experimentally formed by the reaction of Mo back contact with sulfur contained in the absorber precursor (ZnS or SnS) in the case of CZTS solar cell [19]. The next layer was CZTS absorber layer in which most of the incident photons were absorbed to produce electron–hole pairs. CdS or ZnS or $Cd_{0.4}Zn_{0.6}S$ buffer layer was used after that to provide the band alignment between CZTS and following window layer. Afterwards, less costly and available zinc oxide (ZnO) of
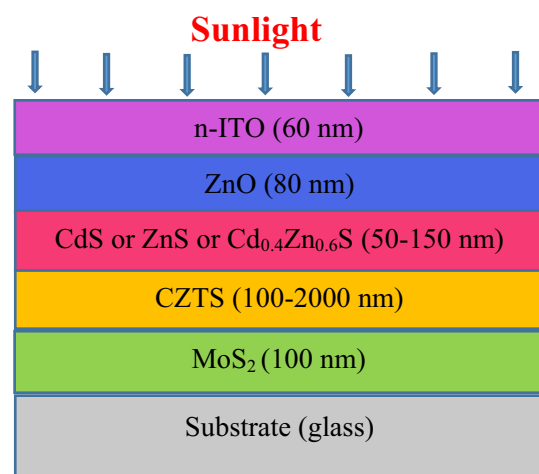

Fig. 1 Structure of CZTS thin-film solar cell

thickness of 80 nm was used for the window layer over the buffer layer which enhances light scattering to enable the efficient use of sun light to maximize the number of incident photons to the buffer and absorber layers [20]. Finally, a transparent conducting film n-type indium tin oxide (n-ITO) of thickness of 60 nm was used to provide a high mobility leading to an increase in visible absorption to obtain a lower sheet resistance [21].

The illumination of light was through the side of n-ITO layer with "Air mass 1.5 global" spectrum with 1000 W/m^2 light power at 25 °C. In this work, the effect of series or shunt resistance was not considered. Two types of single layer defect were introduced in the absorber layer and buffer layer for the simulations. The values of the physical parameters used in this study are all taken from experimental study, different literatures or reasonable estimates [15, 22–25] which are summarized in Table 1.

The observation of CZTS solar cell performances was performed in three different steps. In the first step, the buffer layer's thickness was varied from 50 to 150 nm with equal steps of 25 nm while keeping the absorber layer fixed at 2000 nm. The optimum thickness of the buffer layer was determined and then using it, the performance parameters were calculated and presented for each structure. In the next step, the buffer layer was fixed at its optimum thickness and the CZTS absorber layer was varied for the range of 100–2000 nm with a step size of 400 nm. Then, using the obtained CZTS optimum thickness for their respective buffer layer, the performance parameters were simulated and displayed in this case. Finally, the effect of temperature was observed for each structure by varying the temperature from 290 to 350 K with equal steps of 10 K. It is to be mentioned that for each step the other layers thickness and the material properties were fixed at their respective values.

Results and discussion

Effect of buffer layer's thickness

To investigate the effect of buffer layer's thickness, simulations were done on the structure shown in Fig. 1 with different buffer layers. As already mentioned in Sect. 2, the buffer layer thickness was varied from 50 to 150 nm with a fixed CZTS layer of 2000 nm for the first steps of simulation. A single acceptor-type defect with defect density of 6×10^{16} cm^{-3} was introduced in the buffer layer [25]. Figure 2 shows the variation of solar cell parameters such as open-circuit voltage (V_{oc}), short-circuit current density (J_{sc}), fill factor (FF) and efficiency (η) with the increase in buffer layer thickness. In Fig. 2 (for all graphs), the black line shows the variations for ZnS, the red line (behind the blue line) for CdS and the blue line for Cd$_{0.4}$Zn$_{0.6}$S buffer. In Fig. 2a, the V_{oc} vs. buffer layer thickness is shown where an increasing trend is found for ZnS buffer after 100 nm whereas for CdS and Cd$_{0.4}$Zn$_{0.6}$S, buffer layer change is too small to be found. ZnS buffer layer has higher bandgap with respect to the other two buffer layer for which it acquires larger V_{oc} as larger bandgap decreases diode saturation current. As buffer thickness increases, the amount of photons absorbed outside the hole diffusion length region increases which lowers the recombination rate and thus increases V_{oc} [26]. Next, the change in J_{sc} is shown in Fig. 2b where a decreasing curve is found for ZnS buffer after about 110 nm, on the other hand, curves for other two buffers remain almost flat. When bandgap of a material becomes larger, photons can not achieve the required amount of energy to absorb higher wavelength photons and create electron–hole pair and so result in lower short-circuit current density. That is why

Table 1 The physical parameters of different layer

Parameters	MoS$_2$	CZTS	CdS	ZnS	Cd$_{0.4}$Zn$_{0.6}$S	i-ZnO	n-ITO
Thickness (nm)	100	100–2000	50–150	50–150	50–150	80	60
Bandgap (eV)	1.7	1.5	2.4	3.5	2.98	3.3	3.6
Electron affinity (eV)	4.2	4.5	4.5	4.5	4.2	4.6	4.1
Dielectric permittivity	13.6	10	10	10	9.4	9	10
CB effective density of states (cm^{-3})	2.2×10^{18}	2.2×10^{18}	2.2×10^{18}	1.8×10^{18}	2.2×10^{18}	2.2×10^{18}	2.2×10^{18}
VB effective density of states (cm^{-3})	1.8×10^{19}	1.8×10^{19}	1.8×10^{19}	1.8×10^{19}	1.8×10^{19}	1.8×10^{19}	1.8×10^{19}
Electron thermal velocity (cm s^{-1})	1×10^7	1×10^7	1×10^7	1×10^7	1×10^7	1×10^7	1×10^7
Hole thermal velocity (cm^{-1})	1×10^7	1×10^7	1×10^7	1×10^7	1×10^7	1×10^7	1×10^7
Electron mobility (cm^2/V$_s$)	100	100	100	100	270	100	50
Hole mobility (cm^2/V$_s$)	25	25	25	25	27	25	75
Shallow uniform donor density, N_D (cm^{-3})	0	1×10^1	1×10^{18}	5×10^{15}	1×10^{17}	1×10^{18}	1×10^{19}
Shallow uniform acceptor density, N_D (cm^{-3})	1×10^{16}	2×10^{14}	0	1×10^1	0	0	0
Defect type	–	Donor	Acceptor	Acceptor	Acceptor	–	–
Defect density (cm^{-3})	–	1×10^{13}	6×10^{16}	6×10^{16}	6×10^{16}	–	–

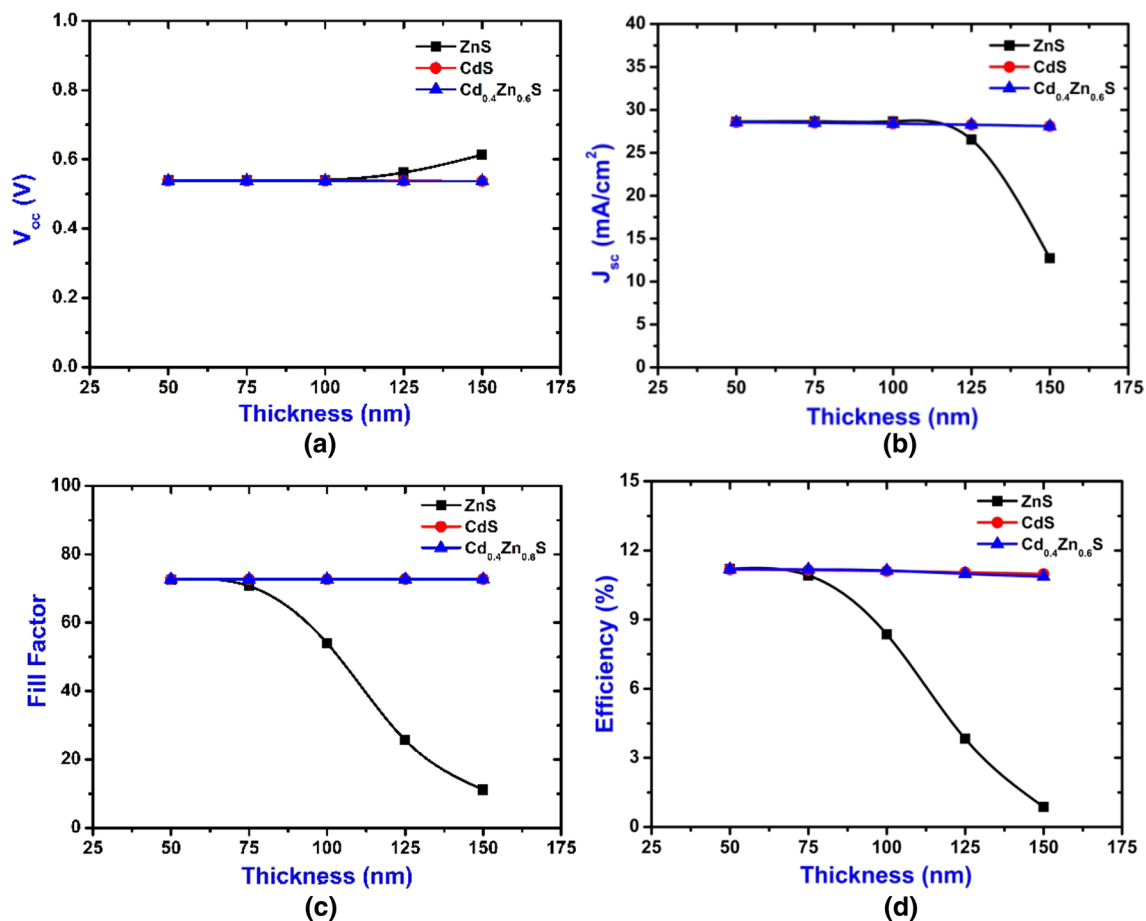**Fig. 2** **a** V_{oc} vs. buffer layer thickness. **b** J_{sc} vs. buffer layer thickness. **c** Fill factor vs. buffer layer thickness. **d** Efficiency vs. buffer layer thickness

ZnS buffer layer possesses lower value of J_{sc} than the two other buffer layers [26]. The decrease in short-circuit density results due to the less production of electron–hole pair as less number of electron–hole pair can reach the absorber layer with increase in buffer layer thickness [22]. In the case of fill factor, the decreasing behavior for ZnS can be seen around 65 nm in Fig. 2c whereas the fill factor for CdS and $Cd_{0.4}Zn_{0.6}S$ do not show any change. The fill factor of ZnS decreases from 65 nm hereafter due to the effect of series resistance which increase with thickness and reduces the maximum achievable power output [27]. Finally, Fig. 2d shows the efficiency curves for the different buffer layers which follow the trend of the fill factor. The efficiency of the solar cell for ZnS buffer layers falls to almost 1% at 150 nm thickness whereas for CdS and $Cd_{0.4}Zn_{0.6}S$ buffers the efficiencies decrease slightly. The efficiencies are changed due to the combined effect of V_{oc}, J_{sc} and fill factor. Note that the solar cell performance can also decrease due to the additional trapping layers created by the defect, which can trap the incident photon [28]. The obtained optimum efficiencies for CdS, ZnS and $Cd_{0.4}Zn_{0.6}S$ buffers are 11.18%, 11.20%

and 11.19%, respectively. The suitable thickness of CdS and $Cd_{0.4}Zn_{0.6}S$ buffer layers is in the range of 50–150 nm, and for ZnS it is the range of 50–75 nm.

Effect of CZTS absorber layer's thickness

The effect of CZTS thickness on solar cell performance was observed through simulations in three different structures CdS/CZTS, ZnS/CZTS and $Cd_{0.4}Zn_{0.6}S$/CZTS. For each simulation, the thickness of CZTS was varied from 100 to 2000 nm with a fixed buffer layer thickness of 50 nm at a temperature of 300 K. A single donor-type defect with a defect density of 1×10^{13} cm^{-3} was introduced in the CZTS layer [25]. Figure 3a–d shows the variation of open-circuit voltage (V_{oc}), short-circuit current density (J_{sc}), fill factor (FF) and efficiency (η), respectively, with increasing absorber layer's thickness. In each figure, the black curve shows the variation for ZnS/CZTS structure, the red curve for CdS/CZTS and the blue curve indicates the $Cd_{0.4}Zn_{0.6}S$/CZTS structure. It is evident from Fig. 3 that all the parameters such as V_{oc}, J_{sc}, FF and η are low at
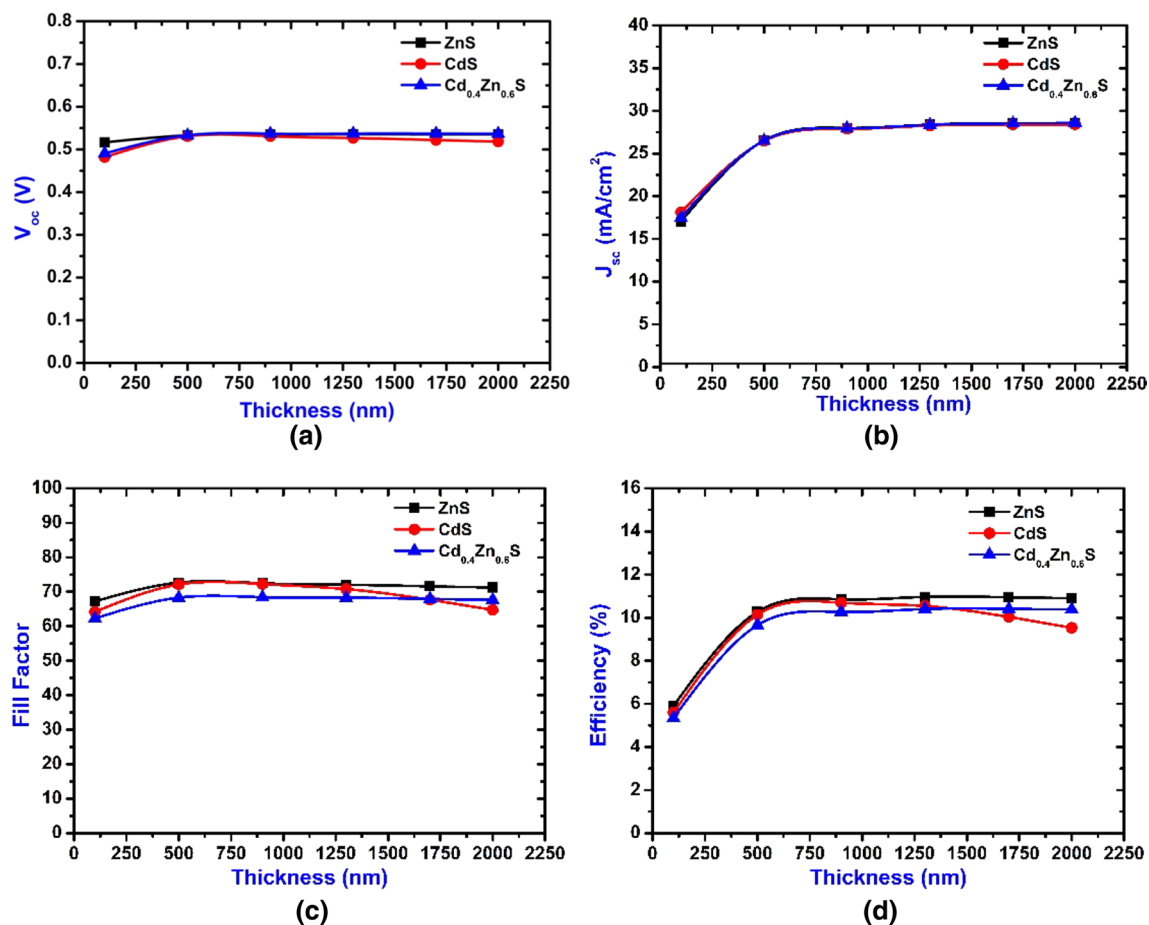
Fig. 3 **a** V_{oc} vs. absorber layer thickness. **b** J_{sc} vs. absorber layer thickness. **c** Fill factor vs. absorber layer thickness. **d** Efficiency vs. absorber layer thickness

lower thickness of CZTS layer (nearly 250–550 nm) which results due to the high recombination of the photo-generated carriers which recombines before reaching the buffer layer/CZTS layer interface [25]. All the parameters then start to increase with the increase in CZTS thickness because the thicker CZTS layer will absorb more photons and generates more electron–hole pairs [25]. But after a certain thickness (900 nm, 1300 nm, and 1700 nm for CdS/CZTS, ZnS/CZTS and $Cd_{0.4}Zn_{0.6}S$/CZTS structures, respectively) the performance again starts to deteriorate as the CZTS layer crosses its minority carrier diffusion length. The decreasing nature can be observed for CdS/CZTS structure clearly whereas for other two structures the decrement is very small to be observed. The incident photons absorbed outside the minority carrier diffusion length are lost by recombination and thus decreases the solar cell performance. The best efficiencies for CdS/CZTS, ZnS/CZTS and $Cd_{0.4}Zn_{0.6}S$/CZTS structures were found 10.69% at 900 nm, 10.96% at 1300 nm and 10.93% at 1700 nm, respectively.

Effect of working temperature

In this section, the effect of temperature was observed for each structure by varying it from 290 K to 350 K. For CdS/CZTS, ZnS/CZTS and $Cd_{0.4}Zn_{0.6}S$/CZTS structures, the CZTS absorber layer's thickness was kept fixed at 900 nm, 1300 nm and 1700 nm, respectively, while the buffer layer's thickness was fixed at 50 nm for every structure. The alteration of open-circuit voltage (V_{oc}), short-circuit current density (J_{sc}), fill factor (FF) and efficiency (η) with increasing temperature is shown Fig. 4 where the black, red and blue lines represent the changes in ZnS/CZTS, CdS/CZTS and $Cd_{0.4}Zn_{0.6}S$/CZTS structures separately. When the temperature increases, there is an increase in the energy of electrons thus the bandgap of the material decreases. The electrons gaining extensive energy thus recombine with other holes. As a result, recombination rate of internal carrier increases resulting in decreasing V_{oc} and efficiency [29]. This effect can be understood quite well from Fig. 4. In Fig. 4a, V_{oc} decreases almost linearly with increasing temperature. This is due to the reverse saturation current which increases with
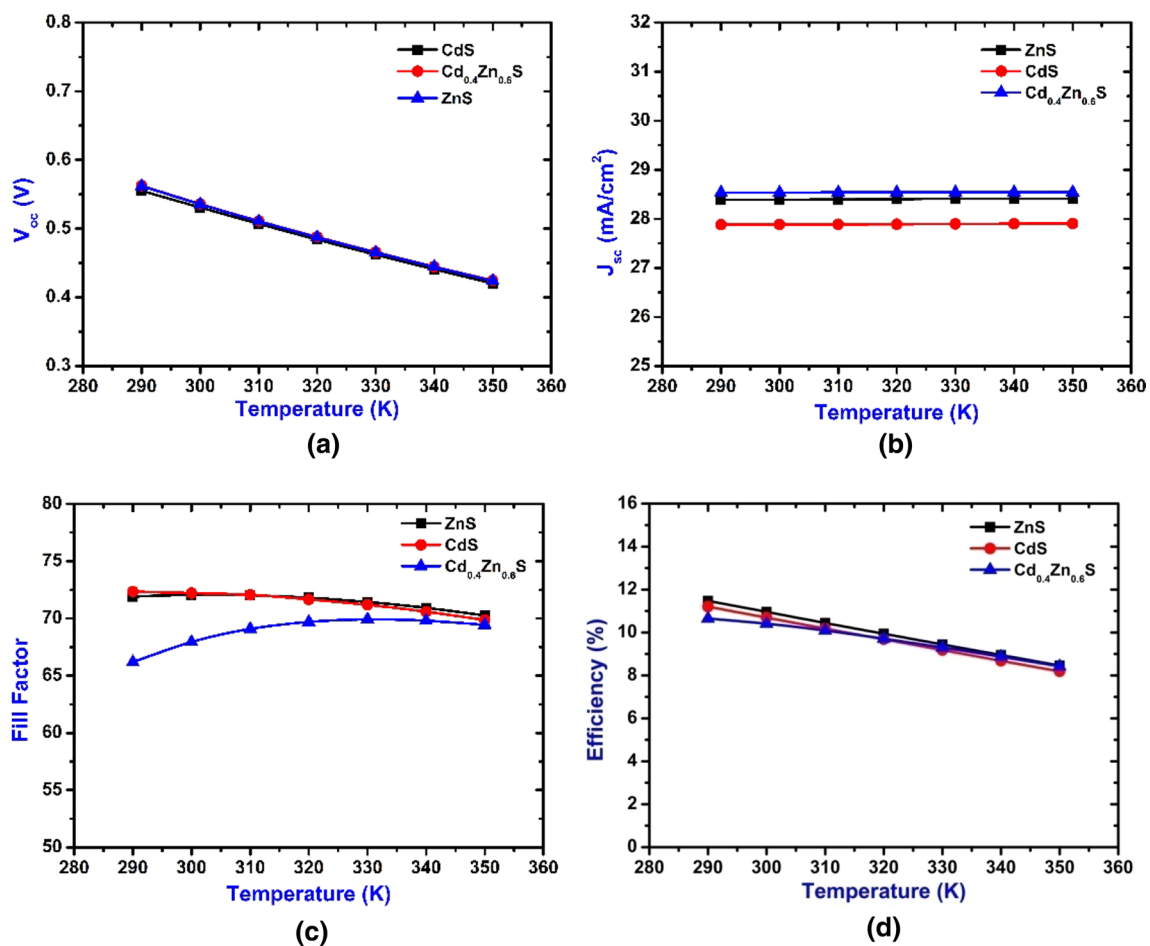
Fig. 4 **a** V_{oc} vs. temperature. **b** J_{sc} vs. temperature. **c** Fill factor vs. temperature. **d** Efficiency vs. temperature

temperature and reduces the saturation current to decrease the open-circuit voltage [22]. The change of J_{sc} is very small with increasing temperature shown in Fig. 4b as recombination process starts to dominate [29]. Whereas the fill factor first increases with temperature as the resistance effect decreases. But it decreases for higher temperature due to light-induced degradation which can be seen from Fig. 4c [29]. Finally, from Fig. 4d, the effect of increase in temperature on solar cell efficiency can be observed which shows a decreasing behavior due to the combined effect of V_{oc}, J_{sc} and fill factor. From the simulation, the best efficiencies for CdS/CZTS, ZnS/CZTS and $Cd_{0.4}Zn_{0.6}S$/CZTS were found 11.20%, 11.47% and 11.58%, respectively, at a temperature of 290 K.

Conclusion

In this work, numerical simulations were performed for CZTS solar cell using three different buffer layers such as CdS, ZnS, and $Cd_{0.4}Zn_{0.6}S$ and the performance

parameters were observed by varying buffer layer thickness, absorber layer thickness and temperature. The buffer layer thickness for all these three types was found 50 nm to obtain high efficiency CZTS solar cell. Among them the CdS buffer layer used in the CZTS solar cell exhibited higher efficiency (11.20%). In all cases performance parameters are affected significantly with the increased buffer layer. Because the loss of incident photons increases with increased buffer thickness which results in lower short circuit density leading to lower efficiency of the solar cell. The lower limit of thickness of CZTS absorber layer was obtained 500 nm to avoid the recombination of photogenerated carriers for all three buffer layers. In contrast the higher limit of thickness of CZTS absorber layer were found 1000 nm, 1400 nm and 1800 nm respectively for CdS, ZnS and $Cd_{0.4} Zn_{0.6}S$ buffer layers to avoid the effect of minority carrier recombination. The best obtained efficiency (10.69%) was found for 900 nm thick CZTS layer using CdS buffer layer. The effect of temperature in CZTS solar cell was also important. In all cases (using different buffer layers) the efficiency decreased if we go beyond 290 K, as in higher temperature there is an

enhancement of internal recombination of photogenerated carriers. The optimization of this study can lead to fabrication of high-efficiency CZTS solar cell.

References

1. Bagher, A.M., Vahid, M.M.A., Mohsen, M.: Types of solar cells and application. Am. J. Opt. Photon. **3**(5), 94–113 (2015)
2. Rao, S., Morankar, A., Verma, H., Goswami, P.: Emerging photovoltaics: organic, copper zinc tin sulphide, and perovskite-based solar cells. J. Appl. Chem. **2016**, 3971579 (2016)
3. Zhao, J., Wang, A., Green, M.A.: 24 5% Efficiency silicon PERT cells on MCZ substrates and 24 7% efficiency PERL cells on FZ substrates. Prog. Photovolt. Res. Appl. **7**(6), 471–474 (1999)
4. Kaur, M., Singh, H.: A review: comparison of silicon solar cells and thin film solar cells. Int. J. Core Eng. Manag. (IJCEM) **3**(2), 15–23 (2016)
5. Green, M.A., Emery, K., Hisikawa, Y., Warta, W., Dunlop, E.D.: Solar cell efficiency tables (Version 49). Prog. Photovolt. Res. Appl. **2017**(25), 3–13 (2016)
6. Yeh, M.Y., Lei, P.H., Lin, S.H., Yang, C.D.: Copper–Zinc–Tin–Sulfur thin film using spin-coating technology. Materials **9**(7), 526 (2016)
7. Katagiri, H., Jimbo, K., Maw, W.S., Takeuchi, A.: Development of CZTS based thin film solar cells. Thin Solid Films **517**(7), 2455–2460 (2009)
8. Wang, W., Winkler, M.T., Gunawan, O., Gokmen, T., Todorov, T.K., Zhu, Y., Mitzi, D.B.: Device characteristics of CZTSSe thin-film solar cells with 12.6% efficiency. Adv. Energy Mater. **4**(7), 1301465 (2014)
9. Maeda, T., Nakamura, S., Wada, T.: Electronic structure and phase stability of in-free photovoltaic semiconductors, $Cu_2ZnSnSe_4$ and Cu_2ZnSnS_4 by first-principles calculation. MRS. Proc. **1165**, https://doi.org/10.1557/PROC-1165-M04-03 (2011)
10. Hironori, K., Kotoe, S., Tsukasa, W., Hiroyuki, S., Tomomi, K., Shinsuke, M.: Development of thin film solar cell based on Cu_2ZnSnS_4 thin films. Sol. Energy Mater. Sol. Cells **65**(1–4), 141–148 (2001)
11. Suryawanshi, M.P., Agawane, G.L., Bhosale, S.M., Shin, S.W., Patil, P.S., Kim, J.H., Moholkar, A.V.: CZTS based thin film solar cells: a status review. Mater. Technol. **28**(1–2), 98–109 (2013)
12. Eisele, W., Ennaoui, A., Schubert-Bischoff, P., Giersig, M., Pettenkofer, C., Krauser, J., Lux-Steiner, M., Zweigart, S., Karg, F.: XPS, TEM and NRA investigations of Zn(Se, OH)/Zn(OH)2 films on Cu(In, Ga)(S, Se)2 substrates for highly efficient solar cells. Sol. Energy Mater. Sol. Cell. **7**(1–2), 17–26 (2003)
13. Nguyen, M., Ernits, K., Tai, K.F., Ng, C.F., Pramana, S.S., Sasangka, W.A., Batabyal, S.K., Holopainen, T., Meissner, D., Neisser, A., Wong, L.H.: ZnS buffer layer for $Cu_2ZnSn(SSe)_4$ monograin layer solar cell. Sol. Energy **111**, 344–349 (2015)
14. Gunavathy, K.V., Parthibaraj, V., Rangasami, C., Tamilarasan, K.: Prospects of alternate buffer layers for CZTS based thin films solar cells from numerical analysis—a review. South Asian J. Eng. Technol. **2**(16), 88–96 (2016)
15. Ferdaous, M.T., Islam, M.F., Haque, K.A.S.M.E., Amin, N.: Numerical analysis of ultra-thin high efficiency $Cd_{1-x}Zn_xS$/$Cd_{1-x}Zn_xTe$ solar cell. Electr. Electron. Eng. **5**(A), 14–18 (2015)
16. Oladeji, I.O., Chow, L., Ferekides, C.S., Viswanathan, V., Zhao, Z.: Metal/CdTe/CdS/$Cd_{1-x}Zn_xS$/TCO/glass: a new CdTe thin film solar cell structure. Sol. Energy Mater. Sol. Cell. **61**, 203–211 (2000)
17. Peter, A.J., Lee, C.W.: Electronic and optical properties of CdS/CdZnS nanocrystals. Chin. Phys. Soc. IOP Publ. **21**(8), 087302 (2012)
18. Niemegeers, A., Burgelman, M., Decock, K., Verschraegen, J., Degrave, S.: SCAPS manual, Version. http://scaps.elis.ugent.be/. Accessed date 19 Dec 2016
19. Yang, K.J., Sim, J.H., Jeon, B., Son, D.H., Kim, D.H., Sung, S.J., Hwang, D.K., Song, S., Khadka, D.B., Kim, J., Kang, J.K.: Effects of Na and MoS_2 on Cu_2ZnSnS_4 thin-film solar cell. Progr Photovolt. Res. Appl. **23**(7), 862–873 (2014)
20. Fuhs, W.: Zinc oxide—a material for micro- and optoelectronic applications. NATO Sci. Ser. II Math. Phys. Chem. **194**, 197–209 (2005)
21. Coutts, T.J., Mason, T.O., Perkins, J.D., Ginley, D.S.: Transparent conducting oxides: status and opportunities in basic research. Electrochem. Soc. Proc. **99–11**, 274–289 (1999)
22. Peijie, L., Lingyan, L., Jinling, Y., Shuying, C., Peimin, L., Qiao, Z.: Numerical simulation of Cu_2ZnSnS_4 based solar cells with In_2S_3 buffer layers by SCAPS-1D. J. Appl. Sci. Eng. **17**(4), 383–390 (2014)
23. Mahbub, R., Islam, M., Anwar, F., Satter, S.S., Ullah, S.M.: Simulation of CZTS thin film solar cell for different buffer layers for high efficiency performance. South Asian J. Eng. Technol. **2**(52), 1–10 (2016)
24. Mebarkia, C., Dib, D., Zerfaoui, H., Belghit, R.: Energy efficiency of a photovoltaic cell based thin films CZTS by SCAPS. J. Fundament. Appl. Sci. **8**(2), 363–371 (2016)
25. Wanda, M.D., Ouédraogo, S., Tchoffo, F., Zougmoré, F., Ndjaka, J.M.B.: Numerical investigations and analysis of Cu_2ZnSnS_4 based solar cells by SCAPS-1D. Int. J. Photoenergy **2016**, 2152018 (2016)
26. Green, M.A.: Solar Cells: Operating Principles, Technologies and System Applications, pp. 86–88. Eaglewood Cliffs, Prentice Hall (1982)
27. Dadu, M., Kapoor, A., Tripathi, K.N.: Effect of operating current dependent series resistance on the fill factor of a solar cell. Sol. Energy Mater. Sol. Cell. **71**(2), 213–218 (2002)
28. Huang, J.Y., Lin, C.Y., Shen, C.H., Shieh, J.M., Da, B.T.: Low cost high-efficiency amorphous silicon solar cells with improved light-soaking stability. Sol. Energy Mater. Sol. Cell. **98**, 277–282 (2012)
29. Green, M.A.: General temperature dependence of solar cell performance and implications for device modeling. Prog. Photovolt. Res. Appl. **11**(5), 333–340 (2003)